AJNR

Regional dynamic signal changes during controlled hyperventilation assessed with blood oxygen level-dependent functional MR imaging.

S Posse, U Olthoff, M Weckesser, L Jäncke, H W Müller-Gärtner and S R Dager

AJNR Am J Neuroradiol 1997, 18 (9) 1763-1770
http://www.ajnr.org/content/18/9/1763

Regional Dynamic Signal Changes during Controlled Hyperventilation Assessed with Blood Oxygen Level–Dependent Functional MR Imaging

Stefan Posse, Uwe Olthoff, Matthias Weckesser, Lutz Jäncke, Hans-Wilhelm Müller-Gärtner, and Stephen R. Dager

PURPOSE: To quantitate the amplitude changes and temporal dynamics of regional functional MR imaging signals during voluntary hyperventilation using blood oxygen level–dependent contrast echo-planar imaging. **METHODS:** Seven male subjects were studied during voluntary hyperventilation ($Petco_2$ = 20 mm Hg) regulated by capnometry. Measurements were made on multisection echo-planar MR images obtained with parameters of 1000/66 (repetition time/echo time), flip angle of 30°, and voxel size of $3 \times 3 \times 5$ mm^3. Sensitivity of the functional MR imaging signal to changes in $Petco_2$, time delays in relation to $Petco_2$ changes, and time constants of functional MR imaging signal changes were assessed on a region-by-region basis. **RESULTS:** Within 20 seconds of starting hyperventilation, rapid and substantial decreases in the functional MR imaging signal (by as much as 10%) were measured in areas of gray matter, which were significantly greater than the modest changes observed in white matter. Regional-specific effects in areas of the frontal, occipital, and parietooccipital cortex were stronger than in subcortical regions or in the cerebellum. Signal decreases measured with functional MR imaging were significantly delayed with respect to the reduction in $Petco_2$. Apparent differences between regional time constants did not reach statistical significance. **CONCLUSION:** Regional and gray–white matter differences in functional MR imaging signal changes during controlled hyperventilation may reflect differences in metabolic activity, vascular regulation, and/or capillary density. When measuring brain activation with functional MR imaging, arterial Pco_2 differences due to unregulated respiration may confound interpretation of activation-related functional MR imaging signal changes.

Index terms: Cerebral blood flow; Magnetic resonance, functional

AJNR Am J Neuroradiol 18:1763–1770, October 1997

Functional magnetic resonance (MR) imaging is increasingly being used to assess cerebral vasomotor reactivity to respiratory challenges and their effect on signal changes in functional MR imaging (1–5) (K. Ying, D. W. Chakeres, P. Schmalbrock, "Functional MRI of Alternating Hyperventilation and Apnea," in: *Abstracts of the Society of Magnetic Resonance,* 1994;4(P): 60; J. V. Hajnal, A. Oatridge, N. Saeed, G. M. Bydder, I. R. Young, "Detection of Changes Produced by Inhalation of Pure Oxygen and Carbogen Using 3D T1-Weighted Brain Imaging," in: *Abstracts of the Society of Magnetic Resonance,* 1995:769; H. B. W. Larsson, E. Rostrup, P. Toft, et al, "fMRI of CO_2 Induced Increase in Cerebral Perfusion," in: *Abstracts of the Society of Magnetic Resonance,* 1993:8; K. K. Kwong, K. M. Donahue, L. Ostergaard, et al, "Mechanism of Brain Signal Increases in Hyperoxia," in: *Abstracts of the Society of Magnetic Resonance* 1995:768). Such studies are of interest because they provide a potential means for characterizing the sensitivity of functional MR contrast to changes in cerebral blood flow (CBF) that are unrelated to changes in blood oxygenation or neuronal activation.

Received January 8, 1997; accepted after revision April 21.

Presented in part at the annual meeting of the American Society of Neuroradiology, Seattle, Wash, June 1996.

From the Institute of Medicine, Research Center Jülich (Germany) GmbH (S.P., U.O, M.W., L.J., H-W.M-G.), and the Departments of Psychiatry and Behavioral Sciences and Bioengineering, University of Washington, Seattle (S.R.D.).

Address reprint requests to Stefan Posse, PhD, Institute of Medicine, Research Center Jülich GmbH, D-52425 Jülich, Germany.

AJNR 18:1763–1770, Oct 1997 0195-6108/97/1809–1763

Voluntary hyperventilation rapidly and strongly reduces CBF, but (except for extreme cases) does not decrease cerebral oxygen consumption in healthy persons (6). As compared with pharmacologic interventions to reduce global CBF, use of voluntary hyperventilation as a physiological challenge has several advantages: it can be carefully monitored and regulated; reduction of global CBF can be induced very rapidly, enabling the time constants of the vascular regulation to be measured; and it can be repeated multiple times in a single experiment to increase sensitivity or to assess reproducibility. If the subject experiences adverse physiological or psychological reactions, controlled hyperventilation can be terminated immediately. The reduction in CBF, which is most pronounced in cortical areas, has been quantitated with positron emission tomography (PET) with oxygen 15 by several research groups (7, 8). In those studies, no specific regional differences in cortical CBF changes were investigated. More recently, Stehling and colleagues (1) have reported hyperventilation-induced cortical signal decreases in blood oxygen level–dependent (BOLD) contrast functional MR imaging. They hypothesized that the observed signal decreases were due to a reduction in cerebral blood volume. A subsequent study by Ying and coworkers, using a strongly flow-sensitized functional MR imaging technique, revealed signal decreases in all cortical vessels after hyperventilation (Ying et al, "Functional MRI..."), consistent with results from Doppler sonographic studies and from ^{15}O PET experiments (7, 8). Our interest in using functional MR imaging to study hyperventilation was stimulated by our previous work using proton echo-planar spectroscopic imaging to measure regional metabolic changes during controlled hyperventilation (9). In that study, we observed global increases in brain lactate in areas of both gray and white matter. The combination of metabolic MR imaging with functional MR imaging may allow the functional relationship between regional metabolic and CBF regulation to be assessed in healthy and diseased brain.

In this study, we specifically assessed the amplitude changes and temporal dynamics of regional functional MR imaging signal change during voluntary hyperventilation using BOLD contrast echo-planar imaging. Hyperventilation was regulated using endtidal CO_2 ($PetCO_2$), which closely parallels arterial CO_2 ($PaCO_2$), to ensure a comparable magnitude of hypocapnia among subjects for measuring functional MR imaging signal changes (10). The amplitudes of the changes in functional MR imaging signals were determined for anatomically defined regions of interest (ROIs), the time delays for these signal changes were determined in relation to $PetCO_2$, and the time constants of the signal changes were computed assuming an exponential signal decay.

Materials and Methods

Seven healthy male subjects (with no known history of vascular disease) were studied 21 times. Written informed consent was obtained in accordance with institutionally reviewed protocols. After baseline measurements were obtained ($PetCO_2$ = 38.1 mm Hg ± 3.5) (all measurements ± standard deviation), subjects were instructed to hyperventilate vigorously. During sustained hyperventilation, which was maintained for up to 3 minutes, $PetCO_2$ was monitored continuously to adjust the respiratory rate to achieve consistent $PetCO_2$ levels of 17.5 ± 2.0 mm Hg (hypocapnia). Expired gas was sampled continuously via a nasal cannula to monitor $PetCO_2$ using a Datex Capnomac (Instrumentarium Corp, Helsinki, Finland) capnometer. In an earlier study, we demonstrated that the $PetCO_2 - PaCO_2$ gradient within subjects is consistent under normal and hypocapnic conditions (10). Measurements were taken with a temporal resolution of between 3 and 5 seconds. There was a $PetCO_2$ measurement delay of approximately 5 seconds after expiration due to dead space from the 7.5 m long cannula.

MR imaging was performed on a clinical 1.5-T whole-body scanner with a maximum gradient amplitude of 25 mT/m and a gradient rise time of 600 milliseconds. The head was secured inside the standard quadrature head coil using tight foam padding. Tapes were placed over the forehead and attached to the head coil to minimize head motion further and to provide a default head position in case head movement occurred. Heart rate was monitored using the pulse oximeter (or the electrocardiogram) unit integrated in the MR scanner. T1-weighted spin-echo imaging was used for anatomic reference and rapid flow-sensitized gradient-echo imaging was used to depict cerebral vasculature.

BOLD contrast functional MR imaging was performed using gradient-echo echo-planar imaging with the following pulse sequence parameters: 1000/66/1 (repetition time [TR]/echo time [TE]/excitations), flip angle of 30°, and voxel size of $3 \times 3 \times 5$ mm^3. The low flip angle was chosen to minimize in-flow effects. Five nonadjacent axial sections from a series of 15 adjacent high-resolution T1-weighted spin-echo images were chosen best to match anatomic structures of interest. The first section was placed in the center of the cerebellum. The second and third sections were placed through the basal ganglia and thalamus (the second section was placed in the high-

resolution imaging section with the largest extension of the thalamus; the third section was placed in the center of the striatum). The fourth section was placed in the centrum semiovale (to exclude artifacts due to cerebrospinal fluid, this section was placed approximately 6 mm above the highest level of the side, or lateral, ventricles). The fifth section was placed in the apex (this section was thought to contain only small parts of white matter and predominantly cortical gray matter). The aim of this section selection was to obtain at least one section for each anatomic structure investigated, where that structure was clearly demarcated. The separation between sections was variable, since each section was matched to individual brain anatomy. Hyperventilation was initiated after 40 seconds of baseline measurements and continued for 60 seconds. The same measurement was repeated after 15 minutes of rest. In addition, three of the seven subjects repeated the protocol on a different day.

To assess whether residual in-flow effects confounded the previous protocol, one of the subjects was retested with a TR of 6000 and a flip angle of 90°. For this study, electrocardiogram gating was used to minimize potentially confounding effects from brain pulsations. Eighteen axial sections covering the cerebrum and part of the cerebellum were acquired. Hyperventilation was initiated after 120 seconds of baseline measurements and continued for 180 seconds. The same measurement was repeated after 15 minutes of rest.

Image registration using the AIR2.0 software developed by Woods et al (11) proved to be difficult for data acquired at a TR of 1000 owing to the large gaps between sections that precluded correction of through-plane motion. Two-dimensional image registration was used to reduce edge artifacts. Data sets were discarded in instances in which gross head displacement could be identified by displaying the images in a cine loop, or in which more subtle head displacement, which correlated with the onset of hyperventilation, could be identified as artifactual signal changes along the edge of the brain and along the ventricles in *z* score images. Two-dimensional image registration was used to reduce edge artifacts in these data sets. Data analysis of reconstructed echo-planar images was performed on a Sun workstation using IDL (Interactive Data Language, Boulder, Colo) and the DPA software package developed by Goldberg and Le Bihan (12). To assess the distribution and strength of regional signal changes visually, we performed a *z* score analysis of the images using a *z* score threshold of two standard deviations.

Anatomically defined ROIs were drawn manually in each hemisphere (Fig 1) in reference to the brain atlas of Talairach and Tourneaux (13); these comprised the frontal cortex, the parietooccipital cortex, the occipital cortex, the cerebellum, the insular cortex, the thalamus, the striatum, and the white matter in the centrum semiovale (averaged over two sections). For data acquired with a TR of 6000, the same ROIs were defined. The functional MR imaging signal intensity data were averaged over the ROIs and then transferred to a PC for further analysis using the Sigmaplot 2.0 software (Jandel Corp, SPSS Inc, Chicago, Ill). The initial seven time points acquired during non–steady-state conditions were discarded.

Analyses using linear regression between the regional functional MR imaging signal intensity values and $Petco_2$ values in each subject were performed to assess the regional sensitivity of the functional MR imaging signal to changes in $Petco_2$ (slope) and the correlation coefficients. Results were averaged over all subjects. The time course of the regional functional MR imaging signals was further analyzed using a nonlinear least squares curve fit routine to calculate four parameters (Fig 2): the signal intensity at rest (S_0), the starting point of the decrease in signal intensity (t_1), the time constant of the decrease in signal intensity (τ), and the signal intensity during maximum hyperventilation (S_1). The fit assumed a constant function during baseline ($t<t_1$):

$$1) \qquad S(t) = S_0$$

and a delayed exponential signal decay during hyperventilation ($t \geq t_1$):

$$2) \qquad S(t) = (S_0 - S_1)\exp(-\tau[t-t_1]) + S_1 .$$

The delay between the decrease in regional functional MR imaging signal and the onset of decreases in global $Petco_2$ (corresponding to a $Petco_2$ decrease that exceeded one standard deviation of baseline fluctuations) was calculated on the basis of t_1 and by taking into account the 5-second $Petco_2$ measurement delay. Results were averaged over all subjects.

Because of the small sample size, the calculated *P* values were used as measures of the size of the effect (14). To detect differences with respect to dependent variables measured in the different brain regions (without relying on statistical artifacts), only effects associated with a *P* value of less than .05 are reported . To assess significance, nonparametric statistical tests (Friedmann's two-way analysis of variance, Wilcoxon's matched-pairs signed rank test) were applied. Correlation coefficients were *z* transformed for comparison of brain regions (15).

Results

Hyperventilation was generally well tolerated; only one subject reported discomfort. To minimize variance due to physiological arousal, data from that subject were discarded from further analysis. Significant out-of-plane head motion precluded data analysis of three measurements obtained in two subjects. The remaining data obtained for 16 measurements in five subjects showed a rapid signal decrease in gray matter areas during the initial 20 seconds of hyperven-

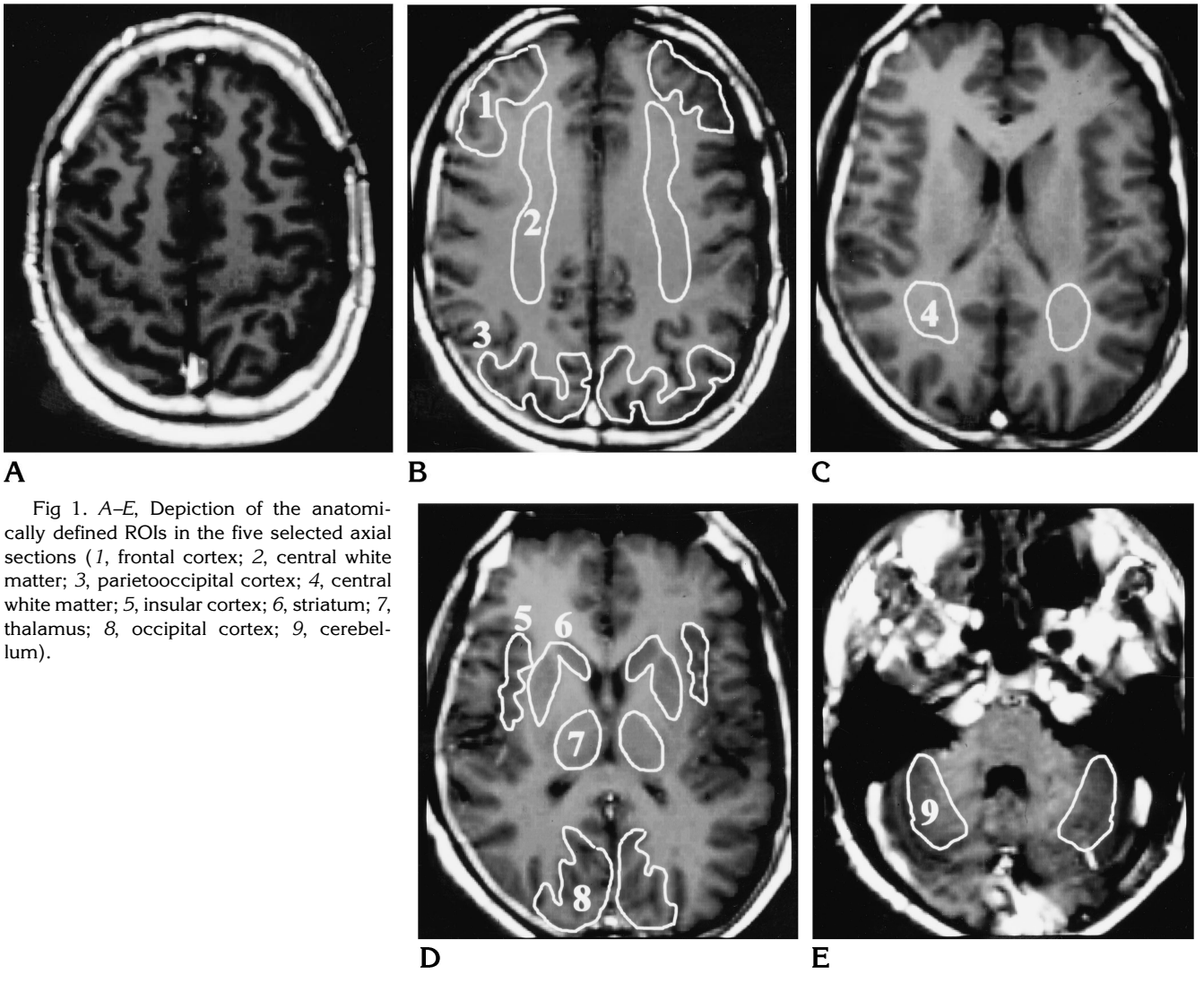

Fig 1. *A–E*, Depiction of the anatomically defined ROIs in the five selected axial sections (*1*, frontal cortex; *2*, central white matter; *3*, parietooccipital cortex; *4*, central white matter; *5*, insular cortex; *6*, striatum; *7*, thalamus; *8*, occipital cortex; *9*, cerebellum).

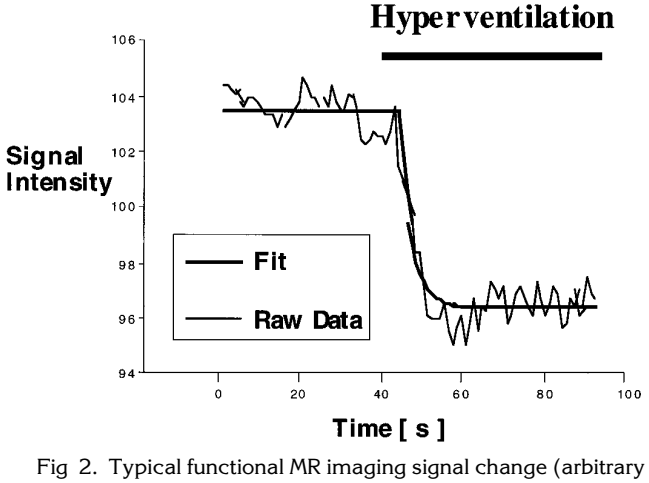

Fig 2. Typical functional MR imaging signal change (arbitrary units) in the occipital cortex with superimposed curve fit. The hyperventilation period is indicated by the horizontal bar.

tilation, which was delayed with respect to the reduction in $P_{ET}CO_2$ (Figs 2–4). In some areas, the change in functional MR imaging signal was detectable within seconds from onset of hyperventilation (Fig 5, Table). The relative signal decreases in parts of the frontal cortex exceeded 10% of baseline. Statistically significant differences ($P = .007$) in signal changes were observed between anatomically defined ROIs (Fig 5, Table). Subsequent analysis (Student-Neuman Keuls method) revealed that white matter had the least sensitivity to changes in Pet_{CO_2}, up to six times less than that in the frontal cortex. In addition, we found that decreases in regional functional MR imaging signal in the insular cortex, the thalamus, the striatum, and the cerebellum were smaller than those in the frontal, parietooccipital, and occip-

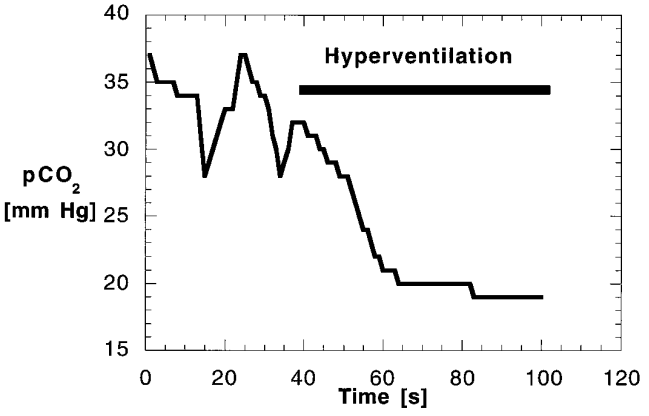

Fig 3. Corresponding time course of the P_{CO_2} change. The hyperventilation period is indicated by the horizontal bar.

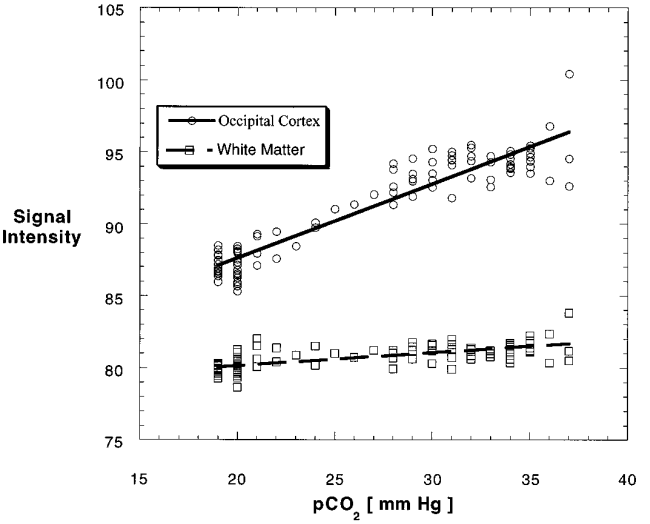

Fig 4. Correlation between functional MR imaging signal changes in the occipital cortex and P_{CO_2}.

ital areas. Although there was a trend toward a between-hemisphere difference in changes in functional MR imaging signal in the frontal cortex, no further statistically significant differences between left and right hemispheres were observed. There were strong linear correlations between Pet_{CO_2} and functional MR imaging signal (z values greater than 1.0), corresponding to a Pearson correlation greater than 0.76 (Fig 5, Table), except for white matter ($P < .002$). Pairwise comparisons using the Student Neuman-Keuls method revealed no significant interregional differences except for white matter.

When assessing the regional temporal dynamics of signal changes (Fig 5, Table), we measured a significant time delay between onset of changes in Pet_{CO_2} and onset of changes in regional functional MR imaging signal for the combined group of ROIs ($P = .009$). Using Dunn's method to investigate individual ROIs, we measured a significant time delay in the cerebellum, the frontal cortex, and white matter (Fig 5). The time constants of the decreases in functional MR imaging signal in areas of gray matter were similar. White matter exhibited a smaller signal decay time constant. Apparent differences between regional time constants did not reach statistical significance ($P = .652$). In some of these data sets, the decreases in functional MR imaging signal were preceded by a slight signal increase during the initial seconds of hyperventilation.

The signal decreases induced by hyperventilation were qualitatively reproducible in all subjects after 15 minutes of rest during the second period of hyperventilation. In well-trained subjects in whom head movement was minimal, even the regional distribution and the magnitude of regional signal changes during repeated hyperventilation were similar (Fig 6). A comparison of the data obtained in one volunteer at TRs of 6000 and 1000 shows that the mean amplitude of signal decreases averaged over all regions at TR of 6000 differed by 1.1% (SD, 2.4%) from those obtained with TR of 1000, suggesting that saturation effects did not significantly confound the observed signal changes with TR of 1000.

Discussion

Hyperventilation results in a number of acute physiological and psychological symptoms, which can include light-headedness, dizziness, visual disturbance, numbness and paresthesia, palpitations, tachycardia, shakiness, tension or anxiety, panic attacks, and weakness or exhaustion (16–18). The immediate physiological effect of hyperventilation is to reduce arterial Pa_{CO_2}, which, in turn, increases perivascular and intraneuronal pH. Increased intraneuronal pH produces a shift in the oxidation/reduction state of central nervous system (CNS) tissue and increases neuronal discharge of both motor and sensory fibers and increases glucose consumption and lactate (and pyruvate) production (9, 10, 19). Rises in perivascular pH induce marked vasoconstriction, which leads to a rapid reduction in CBF, which is observable by functional MR imaging. Our functional MR imaging observations in this preliminary study can be interpreted within the context of currently pro-

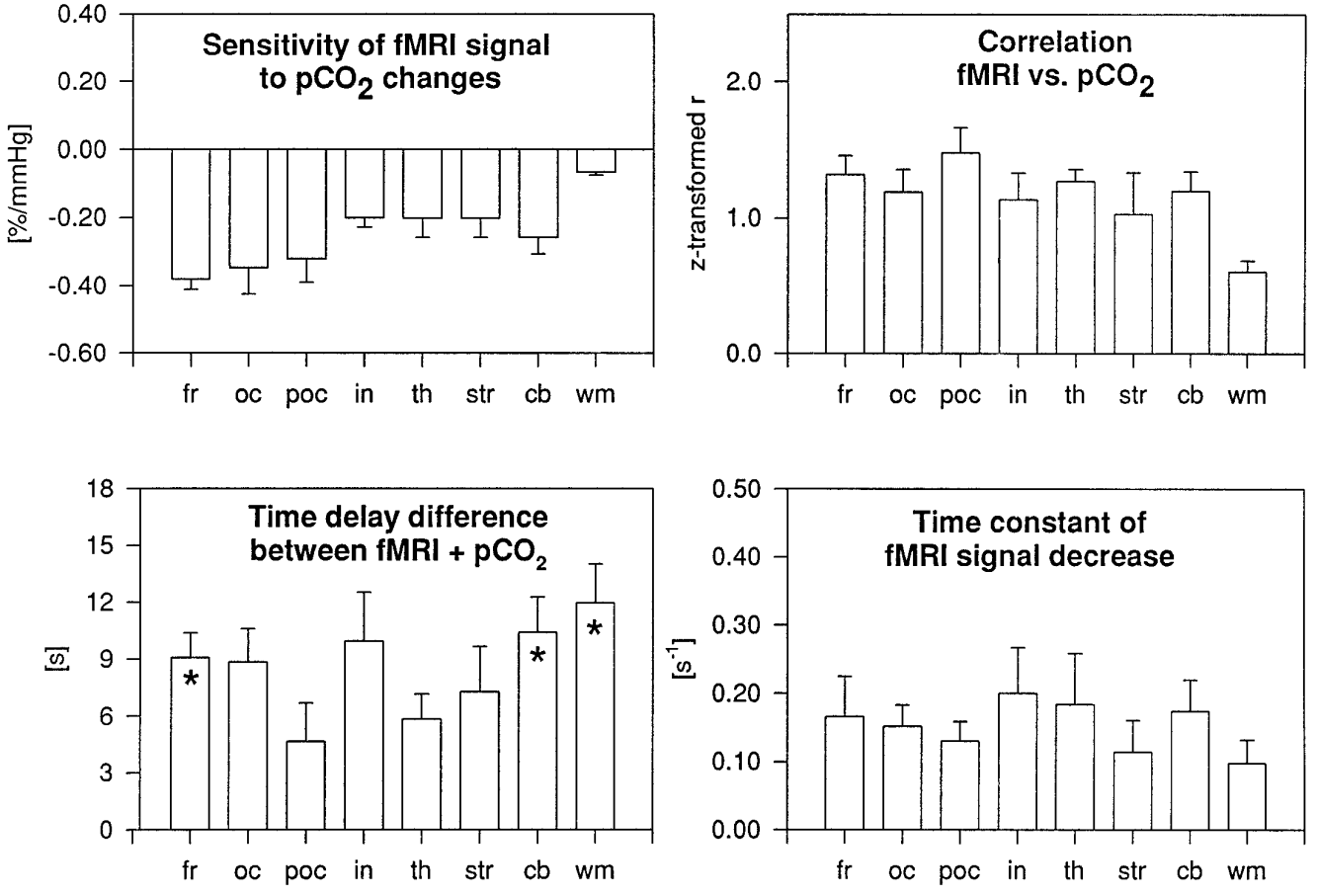

Fig 5. Summary of results (from Table). Error bars indicate standard error of the mean; *asterisk*, $P < .05$; for abbreviations, see Table.

TABLE 1: Regional quantitation of functional MR (fMR) signal dynamics based on 14 measurements in five subjects

Region of Interest	Sensitivity (Linear Regression Slope of fMR Signal vs $Petco_2$), %/mm Hg (SD)	Z-Transformed Correlations: (fMR Signal vs $Petco_2$), (SD)	Time Delay of fMR Signal Decrease with Respect to Start of $Petco_2$ Decrease (Corrected for 5 Second $Petco_2$ Measurement Delay), seconds (SD)	Time Constant of fMR Signal Decrease, s^{-1} (SD)
Frontal cortex	−0.38 (0.18)	1.32 (0.31)	9 (3)	0.17 (0.15)
Occipital cortex	−0.34 (0.20)	1.19 (0.37)	9 (4)	0.15 (0.08)
Parietooccipital	−0.32 (0.17)	1.48 (0.42)	5 (5)	0.13 (0.07)
Cerebellum	−0.26 (0.19)	1.20 (0.33)	10 (4)	0.17 (0.11)
Thalamus	−0.20 (0.14)	1.27 (1.20)	6 (3)	0.16 (0.15)
Striatum	−0.20 (0.12)	1.04 (0.51)	7 (5)	0.11 (0.11)
Insular cortex	−0.20 (0.07)	1.14 (0.43)	10 (6)	0.20 (0.19)
White matter	−0.07 (0.03)	0.61 (0.18)	12 (5)	0.09 (0.07)

Note.—MR imaging performed at TR = 1000.

posed mechanisms thought to be responsible for the BOLD contrast effect (20). To maintain oxidative energy metabolism during blood flow reduction due to hypocapnia, increased oxygen extraction is necessary; this increases the deoxyhemoglobin concentration and reduces the functional MR imaging signal. This interpretation is also consistent with the rise in brain lactate, which we reported in a previous study (9). The apparent regional differences in decreases in functional MR imaging signal in the gray matter, and the much-reduced effect in white matter, may reflect differences in metabolic activity, vascular regulation, and/or capillary density. For example, it is known that the metabolic activity of white matter is approximately three times lower than that of the cortical areas (21). The amplitudes of the functional MR imaging

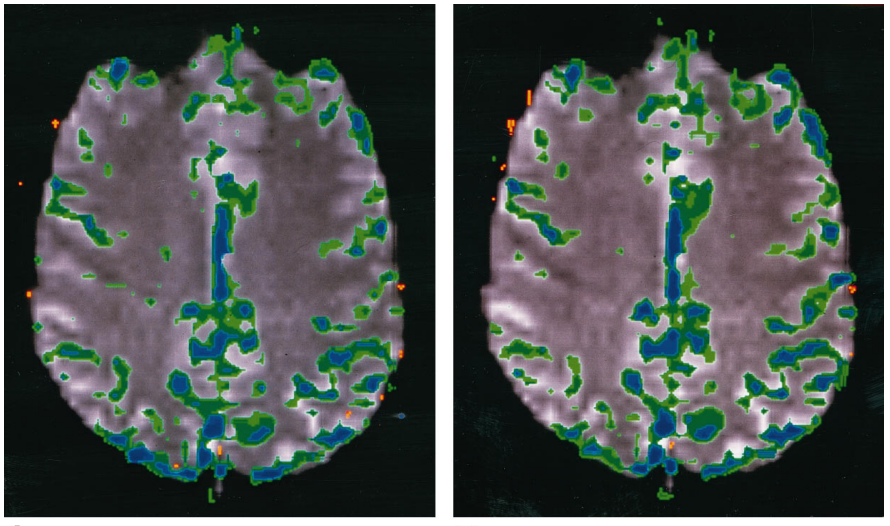

Fig 6. Axial *z* maps of two consecutive hyperventilation periods superimposed on the original echo-planar images (z_{min} = 2.5).

signal changes in insular regions had to be interpreted with caution, since the insular cortex is quite thin and the inclusion of white matter areas was difficult to avoid when drawing the ROI. Temporal characteristics of CBF changes for different brain regions in response to hypocapnia are of theoretical, and potentially of clinical, interest, since they may help to assess regional differences in vascular regulation of clinical conditions, such as vascular disease (22). With the use of high-time-resolution functional MR imaging, it is possible to monitor very rapid signal changes within a few seconds after onset of hyperventilation.

This study underlines the importance of controlling for respiratory changes during functional MR imaging studies of brain activation. In the frontal cortex, which appears to be most sensitive to hypocapnia, as much as a 0.5% change in functional MR imaging signal can be induced by a 1 mm Hg decrease in Pet_{CO_2}. Our previous experience with functional MR imaging indicates that factors such as subject arousal or even slight discomfort may increase respiration, leading to decreases in arterial P_{CO_2}. The confounding effects of arousal or anxiety have been amply demonstrated with other functional imaging techniques, such as single-photon emission computed tomography and PET (23, 24). While simple motor tasks may elicit functional MR imaging signal changes on the order of a few percentage points, higher cognitive functions induce much smaller signal changes, which may be more easily confounded by the effects of unregulated changes in Pet_{CO_2}. The most commonly used analytic method in functional MR imaging, correlational analysis, relies on the temporal signature of the induced signal changes to assess statistical significance. Functional MR imaging signal changes in primary motor and visual brain regions occur relatively rapidly (with time constants on the order of a few seconds) and thereby can be differentiated from the slower signal changes induced by changes in Pet_{CO_2}. However, increasing task complexity may induce a slower change in functional MR imaging signal, which would be difficult to differentiate from signal changes occurring as a consequence of changes in Pet_{CO_2}.

We were unable to use some of the data from two subjects, owing to gross evidence of motion contamination. For retained data sets, it is possible that more subtle head motion contributed to the observed functional MR imaging signal changes during hyperventilation. Although some head motion was difficult to avoid in our study, we would expect that substantial head motion produces increases, as well as decreases, in functional MR imaging signal at the periphery of the brain, along the ventricles, and in other areas with strong image contrast interfaces. In the context of motion artifacts, positive functional MR imaging signal changes should be readily observable, as a large volume of brain between the cerebellum and the centrum semiovale was sampled. In this study, among retained data sets, functional MR imaging signal increases were only observed rarely, and the predominant change was a decrease during hyperventilation. The effects were mostly localized

inside gray matter areas, and the fact that there was a measurable response in white matter argues against predominant motion effects. Signal decreases had regional specificity, which also argues against substantial motion artifacts. However, more subtle head motion may have contributed to individual variability in functional MR imaging signal response. Finally, in contrast to most functional MR imaging studies, we selected rather large ROIs (Fig 1), which are inherently less sensitive to motion artifacts than are small ROIs with focal signal changes.

In conclusion, the use of BOLD functional MR imaging to assess CBF changes during hyperventilation may help to elucidate mechanisms involved in regional metabolic and vascular regulation and to broaden our understanding of CNS disease processes that affect those regulatory mechanisms. Previous work has shown that functional MR imaging signal changes in the visual cortex are reduced when CBF is increased (25). Decreases in CBF arising from uncontrolled hypocapnia also may reduce the sensitivity of functional MR imaging for detecting brain activation.

Acknowledgments

We thank Denis Le Bihan (Orsay, France) for sharing his functional MR imaging analysis software package and Edgar Müller (Siemens AG, Germany) for making available a pre-release of his echo-planar pulse sequences. We also thank Wolfgang Klement (University of Düsseldorf, Institute of Clinical Anaesthesiology) for providing the Datex Capnomac CO_2 monitor. Software support for the nonlinear curve fit was provided by Paul Jansen (Central Institute of Applied Mathematics, Research Center Jülich GmbH) and by Frank Sonnenberg (Institute of Medicine, Research Center Jülich GmbH).

References

1. Stehling MK, Turner R, Mansfield P. Echo-planar imaging: magnetic resonance imaging in a fraction of a second. *Science* 1991; 254:43–50
2. Kwong KK, Wanke I, Donahue KM, Davis TL, Rosen BR. EPI imaging of global increase of brain MR signal with breath-hold preceded by breathing O_2. *Magn Reson Med* 1995;33:448–452
3. Stillman AE, Hu X, Jerosch-Herold M. fMRI of brain during breath holding at 4T. *Magn Reson Imaging* 1995;13:893–897
4. Rostrup E, Larsson HB, Toft PB, et al. fMRI of CO_2 induced increase in cerebral perfusion. *NMR Biomed* 1994;7:29–34
5. Moseley ME, Chew WM, White DL, et al. Hypercarbia-induced changes in cerebral blood volume in the cat: a ^1H MRI and intravascular contrast agent study. *Magn Reson Med* 1992;23:21–30
6. Van Rijen PC, Luyten PR, Berkelbach Van Der Sprenkel JW, et al. ^1H and ^{31}P NMR measurement of cerebral lactate, high-energy phosphate levels and pH in humans during voluntary hyperventilation: associated EEG, capnographic, and Doppler findings. *Magn Reson Med* 1989;10:182–193
7. Bednarczyk EM, Rutherford WF, Leisure GP, et al. Hyperventilation-induced reduction in cerebral blood flow: assessment by PET. *Ann Pharmacother* 1990;24:456–459
8. Ramsay SC, Murphy K, Shea SA, et al. Changes in global cerebral blood flow in humans: effect on regional cerebral blood flow during a neural activation task. *J Physiol* 1993;471:521–534
9. Posse S, Dager S, Richards T, et al. In vivo measurement of regional brain metabolic response to hyperventilation using magnetic resonance proton echo planar spectroscopic imaging (PEPSI). *Magn Reson Med* 1997;37:858–865
10. Dager SR, Strauss WL, Marro KI, Richards TL, Metzger GD, Artru AA. Proton magnetic resonance spectroscopic investigation of hyperventilation in subjects with panic disorder and comparison subjects. *Am J Psychiatry* 1995;152:666–672
11. Woods RP, Mazziotta JC, Cherry SR. Automated image registration. In: Uemura K, Lassen NA, Jones T, Kanno L, eds. *Quantification of Brain Function: Tracer Kinetics and Image Analysis in Brain PET*. Amsterdam, the Netherlands: Elsevier; 1993;:391–398
12. Le Bihan D. Integrated processing software for functional MRI. *Human Brain Mapping* 1995;supp 1:151
13. Talairach J, Tournaux P. *Coplanar Stereotaxic Atlas of the Human Brain*. New York, NY: Thieme Medical; 1988
14. Krauth J. *Distribution-Free Statistics: An Application-Oriented Approach*. Amsterdam, the Netherlands: Elsevier; 1988
15. Sachs L. *Angewandte Statistik*. Berlin, Germany: Springer-Verlag; 1984
16. Belmer H, Haardonk H. Symptomatik und Behandlung des Hyperventilations Syndroms. *Mnch Med Wschr* 1971;113: 1255–1258
17. Hill O. The hyperventilation syndrome. *Br J Psychiatry* 1979;135: 367–368
18. Lum LC. Hyperventilation and anxiety state (editorial). *J R Soc Med* 1981;74:1–4
19. Siesjo BK. Carbon dioxide in brain energy metabolism. In: Siesjo BK, ed. *Brain Energy Metabolism*. New York, NY: Wiley; 1978: 288–323
20. Boxermann JL, Hamberg LM, Rosen BR, Weisskopf RM. MR contrast due to intravascular magnetic susceptibility perturbations. *Magn Reson Med* 1995;34:555–566
21. Siesjo BK. Regional metabolic rates in the brain. In: Siesjo BK, ed. *Brain Energy Metabolism*. New York, NY: Wiley; 1978: 131–150
22. Ringelstein EB, Sievers C, Ecker S, Schneider PA, Otis SM. Noninvasive assessment of CO_2-induced cerebral vasomotor response in normal individuals and patients with internal carotid artery occlusions. *Stroke* 1988;19:963–969
23. Gur RC, Gur RE, Resnick SM, Skolnick BE, Alavi A, Reivich M. The effect of anxiety on cortical cerebral blood flow and metabolism. *J Cereb Blood Flow Metab* 1987;7:173–177
24. Dager SR, Layton ME, Richards TL. Neuroimaging findings in anxiety disorders. *Semin Clin Neuropsychiatry* 1996;1:48–60
25. Bruhn H, Kleinschmidt A, Boecker H, Merboldt K-D, Hnicke W, Frahm J. The effect of acetazolamide on regional cerebral blood oxygenation at rest and under stimulation as assessed by MRI. *J Cereb Blood Flow Metab* 1994;14:742–748